Spin correlation parameter C_{yy} of p+^{3}He elastic backward scattering

Y. Shimizu,[1,*] K. Hatanaka,[1] Y. Tameshige,[1] T. Adachi,[1] K. Fujita,[1] H. Matsubara,[1] H. Okamura,[1] A. Tamii,[1] A. P. Kobushkin,[2] T. Kawabata,[3] Y. Sasamoto,[3] K. Suda,[1,3] T. Uesaka,[3] K. Itoh,[4] Y. Sakemi,[5] T. Wakui,[5] M. Uchida,[6] T. Kudoh,[7] K. Sagara,[7] T. Wakasa,[7] H. P. Yoshida,[8] Y. Shimbara,[9] E. A. Strokovsky,[10] S. Ishikawa,[11] and M. Tanifuji[11]

[1]*Research Center for Nuclear Physics (RCNP), Osaka University, Ibaraki, Osaka 567-0047, Japan*
[2]*N. N. Bogolyubov Institute for Theoretical Physics, 252143 Kiev, Ukraine*
[3]*Center for Nuclear Study (CNS), University of Tokyo, Wako, Saitama 351-0198, Japan*
[4]*Department of Physics, Saitama University, Urawa, Saitama 338-8570, Japan*
[5]*Cyclotron and Radioisotope Center (CYRIC), Tohoku University, Sendai, Miyagi 980-8578, Japan*
[6]*Department of Physics, Tokyo Institute of Technology, Oh-okayama, Meguro, Tokyo 152-8550, Japan*
[7]*Department of Physics, Kyushu University, Hakozaki, Fukuoka 812-8581, Japan*
[8]*Research and Development Center for Higher Education, Kyushu University, Ropponmatsu, Fukuoka 810-8560, Japan*
[9]*NSCL, Michigan State University, East Lansing, Michigan 48824, USA*
[10]*Joint Institute for Nuclear Research, RU-141980 Dubna, Russia*
[11]*Department of Physics, Science Research Center, Hosei University, Fujimi, Tokyo 102-8160, Japan*

(Received 2 May 2007; published 8 October 2007)

We measured the differential cross section and the spin correlation parameter C_{yy} of the $\vec{p}$+$^3\vec{\text{He}}$ elastic backward scattering at 200, 300, and 400 MeV at $\theta = 180^\circ$ in the center-of-mass frame to study the mechanism of the reaction and to examine the validity of the ^{3}He wave functions based on two different realistic two-body forces. This is the first measurement of the spin correlation parameter C_{yy} of the $\vec{p}$+$^3\vec{\text{He}}$ EBS at intermediate energies. The experimental results were compared with few-body calculations, including three reaction mechanisms: two-nucleon-pair exchange, pion exchange, and direct pp scattering. It was found that few-body calculations describe the differential cross-section data reasonably well. The spin correlation parameter C_{yy} shows clear evidence for the two-nucleon-pair exchange processes in the reaction, demonstrating that the spin observables are helpful for deeper understanding of the reaction mechanism.

DOI: 10.1103/PhysRevC.76.044003 PACS number(s): 21.45.+v, 24.70.+s, 25.10.+s, 29.25.Pj

I. INTRODUCTION

In the past decades intensive effort has been dedicated to the investigation of the structure of the lightest nuclei (d, ^{3}He, ^{4}He) at short distances between constituent nucleons. Since high-quality data on spin-dependent observables became available [1–6], significant progress has been achieved both experimentally as well as theoretically. Largely, these studies used proton elastic backward scattering (EBS) off nuclei at $\theta = 180^\circ$ in the center-of-mass frame. The EBS involves a large-momentum transfer and the process is expected to probe the high-momentum components of the wave functions of the lightest nuclei.

The structure of the ^{3}He nucleus was investigated using the ^{3}He(p, $2p$) and ^{3}He(p, pd) reactions at TRIUMF [7]. It was found that calculations using realistic 2N potentials are unable to reproduce the measured nucleon momentum distribution in the region of internal momentum $q > 300$ MeV/c. To investigate the spin structure of ^{3}He, spin correlations for the quasielastic $^3\vec{\text{He}}(\vec{p}, pN)$ reaction were measured as a function of the transferred momentum at IUCF [8]. However, Faddeev calculations did not reproduce measured nucleon polarization data in the region of $q > 300$ MeV/c. In summary, the structure of the ^{3}He nucleus at high momenta is not been clearly understood yet. The EBS may provide a tool to obtain this information on the structure of the ^{3}He nucleus because of its high momentum transfer nature. The p+^{3}He EBS, however, has been studied in much less detail than the p+d EBS. To find an adequate connection of this process with the structure of the ^{3}He and to get quantitative estimations for sensitivities of its cross section and spin-dependent observables to the existing ^{3}He wave functions, studies of the reaction mechanism are urgently needed, especially at intermediate energies.

Recently, the p+^{3}He EBS has been analyzed [9–11] on the basis of the distorted-wave Born approximation (DWBA) using the 3N bound state wave function obtained by solving the Faddeev equation. Uzikov *et al.* [11] have calculated the differential cross section of the p+^{3}He EBS based on two reaction mechanisms. One is the sequential transfer (ST) of a proton-neutron pair, and the other is the mechanism related to the excitation of nucleon isobars in the intermediate states followed by the exchange of virtual pions between the isobars and the nucleons (OPE). It was found that the ST is the major process at low ($E_p < 0.3$ GeV) and high ($E_p > 1.0$ GeV) energies. However, the ST process has the minimum cross section around 0.4 GeV and the OPE mechanism shows a dominant contribution at energies between 0.3 and 0.8 GeV. It is of interest to investigate the relative importance of ST and OPE contributions to the EBS in this energy region. It has been pointed out that the OPE mechanism that was considered

*Corresponding author: CNS, University of Tokyo, Wako, Saitama 351-0198, Japan; yshimizu@cns.s.u-tokyo.ac.jp

is not T invariant [12]. To remove the physical inaccuracies, Kobushkin *et al.* introduced the pion-exchange mechanism based on a two-loop diagram [13]. They showed sensitivities of the spin observables on the ^{3}He wave functions. Although their calculations were limited by not including entrance and exit channel distortions, spin observables are generally less sensitive to distortions than the cross sections for which large distortion effects were reported by Uzikov *et al.* [11].

To extract more detailed information on the reaction mechanism, rigorous numerical calculations of spin-dependent observables as well as the cross section are needed. However, until now no data existed for the spin-dependent observables of the p+^{3}He EBS at intermediate and high energies. A high-intensity beam of polarized protons in combination with a polarized ^{3}He target would give a unique opportunity for detailed studies of p+^{3}He EBS, including the spin-dependent observables. Because vector-analyzing power vanishes at $\theta = 180^\circ$ in the center-of-mass frame, we measured the differential cross section and the spin correlation parameter C_{yy} of the p+^{3}He EBS at 200, 300, and 400 MeV to study the reaction mechanisms and the ^{3}He wave function. In particular, the reaction mechanism, including the pion exchange, would give information on the non-nucleonic degrees of freedom in the wave function of the target nucleus. Both the cross section and C_{yy} will be helpful for a better understanding of the structure of the ^{3}He at high momenta.

The measurements of the differential cross section and the spin correlation parameter C_{yy} of the p+^{3}He EBS are described in Sec. II. To perform the spin-correlation experiments, it was indispensable to develop a polarized target as well as a polarized beam. We describe the polarized ^{3}He target developed in this work in Sec. II. The theoretical predictions are summarized in Sec. III, and the experimental results are compared with the theoretical predictions in Sec. IV. A summary is given in Sec. V.

II. EXPERIMENTAL METHOD

The measurements of the $\vec{p}$+$^3\vec{\text{He}}$ EBS were performed at the Research Center for Nuclear Physics (RCNP), Osaka University. Polarized protons produced in an atomic beam polarized ion source [14] were accelerated by the $K = 140$ MeV AVF (azimuthally varying field) cyclotron up to 39.3, 53.3, and 64.2 MeV. The proton beam was then accelerated up to 200, 300, and 400 MeV, respectively, by the $K = 400$ MeV ring cyclotron. The extracted beam was transported [15] to the polarized ^{3}He gas target at the center of the scattering chamber of the magnetic spectrometer Grand Raiden (GR) [16], which was used to analyze the scattered particles at 0°. Figure 1 shows the schematic layout of the GR spectrometer and its focal plane (FP) detectors. To stop the beam and integrate the beam current, Faraday cups (FC1 and FC2) were installed inside the first dipole magnet of the GR spectrometer as shown in Fig. 1. The first Faraday cup was used in the measurements of the $^3\vec{\text{He}}(\vec{p}, \pi^+)^4$He reaction to determine the ^{3}He polarization, and the second cup FC2 was used in the measurements of the $\vec{p}$+$^3\vec{\text{He}}$ EBS. Typical beam intensities were 10 to 40 nA, limited by acceptable counting rates in the detectors. The beam

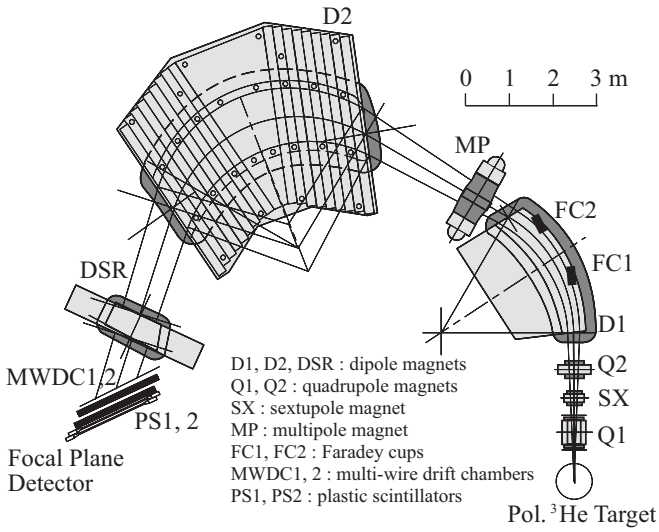

FIG. 1. Schematic view of the high-resolution spectrometer Grand Raiden at RCNP.

polarization was monitored by two beam-line polarimeters in the West Experimental hall. During the measurements, the beam polarization was typically 0.70.

A. Polarized ^{3}He target

A spin-exchange-polarized ^{3}He target [17] was used to perform the spin-correlation measurements. The method to polarize a ^{3}He nucleus is based on the principle of optical pumping of Rb vapor and spin-exchange collisions with ^{3}He gas. A schematic view of the major components of the target is shown in Fig 2. The target consisted of a double chamber including the target and the optical pumping chamber, connected by a thin transfer tube. The design prevents depolarization of the Rb vapor by the proton beam. The target cell contained the ^{3}He gas with a density of 9.8×10^{19} atoms/cm^3 together with a small amount of N_2 gas and Rb vapor. During operation, the pumping chamber was heated to about 460 K to provide a sufficiently high Rb vapor density and maintain the polarization of the ^{3}He gas. About 60 W of circularly polarized photons were used to optically pump Rb. Polarized ^{3}He nuclei were allowed to diffuse into the target chamber. The target cell was made of borosilicate glass (Corning 7056) known to have a very long relaxation time for the polarization of ^{3}He. The target cell had a diameter of 5 cm and was 10 cm long in beam direction. The windows of the target chamber were made as thin as 100 μm to reduce background produced in the windows.

During the $\vec{p}$+$^3\vec{\text{He}}$ measurements, the ^{3}He polarization was monitored for 40 s every hour by the adiabatic fast passage (AFP) NMR method. A single experimental run was typically 1.5 h long. The direction of the polarization was reversed every other run, i.e., every 3 h. The NMR signals gave relative values of the polarization. The absolute value of the target polarization was determined by a calibration using the $^3\vec{\text{He}}(\vec{p}, \pi^+)^4$He reaction. In the special case of this reaction with spin parities of $\frac{1}{2}^+ + \frac{1}{2}^+ \rightarrow 0^- + 0^+$, where the parity changes, one can show

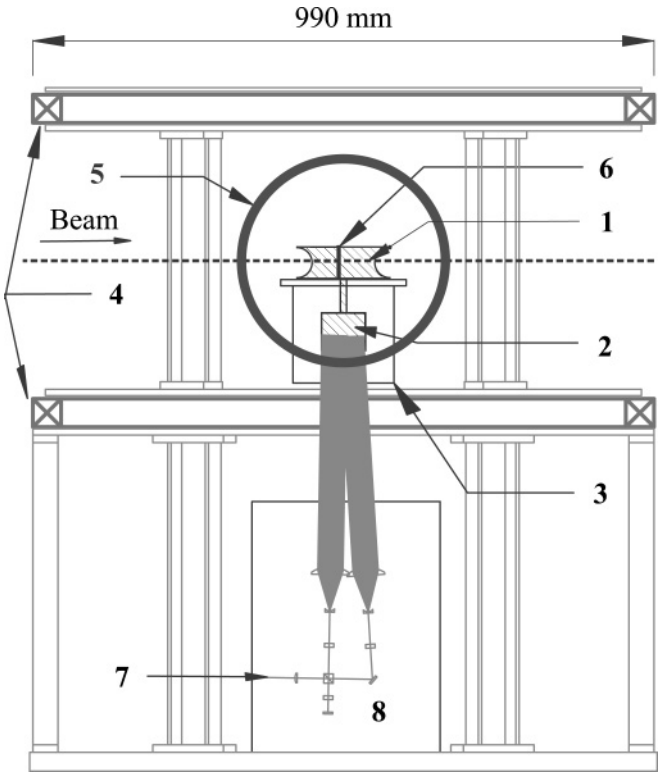

FIG. 2. Schematic view of the polarized ^{3}He target system. 1, target chamber; 2, pumping chamber; 3, oven; 4, main coil; 5, RF coil; 6, pick-up coil; 7, diode laser; 8, optical elements. The hatched parts are the target chamber (upper) and the pumping chamber (lower), coupled together by a thin drift tube.

that the spin-correlation parameter C_{yy} has a constant value of $+1$ [18]. The measured target polarization was typically $p_y^T = 0.19$ with a systematic uncertainty of $\Delta p_y^T / p_y^T = 6\%$ due to the uncertainties of the proton beam polarization. A more detailed description of the polarized target will be given elsewhere [19].

B. Cross section and spin correlation parameter

The outgoing ^{3}He particles in the $\vec{p}+\vec{^3\mathrm{He}}$ EBS were momentum analyzed by the GR spectrometer set at 0°. The scattered particles were magnetically analyzed and focused in the focal plane (FP). The FP detector system consisted of two sets of the multiwire drift chambers MWDC1 and MWDC2 [20] followed by two plastic scintillation counters PS1 and PS2 (see Fig. 1). Event triggers for data acquisition [21] were generated by a coincidence of signals from the two plastic scintillators. The trajectories of the particles were reconstructed using the positions measured in the two MWDCs.

The large number of particles scattered from the Faraday cup (FC2) in the spectrometer magnet D1 (see Fig. 1) caused serious background in the measurement of the $\vec{p}+\vec{^3\mathrm{He}}$ EBS. To distinguish reaction events from background, particle identification was carried out using the energy loss from the PS1 and PS2 scintillators. In addition, the reconstruction of the particle trajectory in the MWDCs was included in the particle identification, since most of the X- and γ-ray background events did not make tracks in the wire chambers.

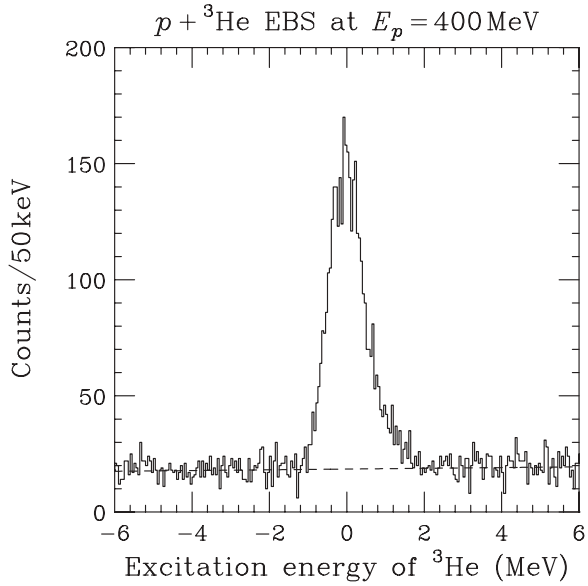

FIG. 3. Typical excitation energy spectrum of the $\vec{p}+\vec{^3\mathrm{He}}$ EBS at 400 MeV. The dashed curve shows the fitting result of the background events.

Figure 3 shows an example of the typical excitation energy spectra of the $\vec{p}+\vec{^3\mathrm{He}}$ EBS at 400 MeV. The energy resolution was 870 keV in full width at half maximum at 400 MeV. The ^{3}He particles from the $SiO_2(p, {}^3\mathrm{He})$ reaction in the glass cell window showed a nearly flat distribution in the energy spectrum. This smooth background was estimated by fitting a linear function in energy to the data outside of the peak. The shape of the peak was assumed to be a Gaussian with an exponential tail. The yields were obtained by integrating the fitted functions.

Assuming that the strong interaction is symmetric under parity and time reversal, the spin-dependent cross section for a scattering of a spin-$\frac{1}{2}$ projectile by a spin-$\frac{1}{2}$ target is given by [18]

$$\sigma = \sigma_0\left(1 + p_y A_y + p_y^T A_y^T + p_y p_y^T C_{yy}\right), \tag{1}$$

where σ_0 is the spin-independent cross section, and p_y and p_y^T are the beam and the target polarizations, respectively. In the present experiment, both the beam and the target polarizations were pointed in the vertical direction. The measured yields of the four possible spin combinations of the beam and the target are expressed as follows

$$Y_{\uparrow\uparrow} = \sigma_0\left(1 + p_y A_y + p_y^T A_y^T + p_y p_y^T C_{yy}\right), \tag{2}$$

$$Y_{\uparrow\downarrow} = \sigma_0\left(1 + p_y A_y - p_y^T A_y^T - p_y p_y^T C_{yy}\right), \tag{3}$$

$$Y_{\downarrow\uparrow} = \sigma_0\left(1 - p_y A_y + p_y^T A_y^T - p_y p_y^T C_{yy}\right), \tag{4}$$

$$Y_{\downarrow\downarrow} = \sigma_0\left(1 - p_y A_y - p_y^T A_y^T + p_y p_y^T C_{yy}\right), \tag{5}$$

where Y is the measured yield normalized to the charge measured in FC2, the target thickness and the solid angle of the GR spectrometer. The solid angle was 2.8 msr. Vertical

TABLE I. Measured cross sections $d\sigma/d\Omega$ and spin correlation parameter C_{yy} of the $\vec{p}+\vec{^3\mathrm{He}}$ EBS in the center-of-mass frame. Only statistical errors are shown.

Energy (MeV)	$d\sigma/d\Omega$ (μb/sr)	C_{yy}
200	14.2 ± 0.1	-0.056 ± 0.020
300	3.56 ± 0.01	0.168 ± 0.048
400	2.04 ± 0.01	0.336 ± 0.052

slits were installed at ± 35 mr, and the horizontal angular opening was determined by off-line analysis. The first and second arrows (up or down) in a subscript indicate the spin directions of the beam and the target, respectively. From these equations, the differential cross section and spin correlation parameter C_{yy} are obtained as

$$\left(\frac{d\sigma}{d\Omega}\right)_{\mathrm{lab}} = \frac{1}{4}\left(Y_{\uparrow\uparrow} + Y_{\uparrow\downarrow} + Y_{\downarrow\uparrow} + Y_{\downarrow\downarrow}\right), \tag{6}$$

$$C_{yy} = \frac{1}{p_y p_y^T}\frac{1 - A_C}{1 + A_C}, \tag{7}$$

where

$$A_C \equiv \frac{Y_{\uparrow\downarrow} + Y_{\downarrow\uparrow}}{Y_{\uparrow\uparrow} + Y_{\downarrow\downarrow}}. \tag{8}$$

Experimental results thus derived are listed in Table I. Only statistical errors are shown. Systematic uncertainties for $d\sigma/d\Omega$ and C_{yy} are estimated to be 5 and 8%, respectively. The uncertainties in the cross section and C_{yy} are mainly due to errors in the density and the polarization of the ^{3}He target, respectively.

III. THEORETICAL FORMALISM

Before a comparison of the experimental results with the rigorous calculations made by Kobushkin *et al.*, the theoretical treatment is briefly summarized in the following. The amplitude for the elastic scattering of two spin $\frac{1}{2}$ particles consistent with the parity and time reversal invariance includes six independent complex amplitudes. In the case of $\vec{p}+\vec{^3\mathrm{He}}$ scattering at $\theta = 180^\circ$ in the center-of-mass frame, only three independent amplitudes remain. If we write the scattering amplitudes as $M_{Mm}^{M'm'}$, with M, m and M', m' as magnetic quantum numbers of ^{3}He and proton in the initial and the final states, respectively, the three independent amplitudes are

$$A \equiv M_{++}^{++} = M_{--}^{--}, \tag{9}$$

$$F \equiv M_{+-}^{+-} = M_{-+}^{-+}, \tag{10}$$

$$G \equiv M_{+-}^{-+} = M_{-+}^{+-}. \tag{11}$$

With these amplitudes, the two observables can be expressed as

$$\frac{d\sigma}{d\Omega} = \frac{|A|^2 + |F|^2 + |G|^2}{128\pi^2 s}, \tag{12}$$

$$C_{yy} = \frac{2\mathrm{Re}(FG^*)}{|A|^2 + |F|^2 + |G|^2}, \tag{13}$$

where s is the square of the total center-of-mass energy.

Kobushkin *et al.* have taken into account the three reaction mechanisms [13] that are shown in Fig. 4. The first (A) is the exchange of a two-nucleon pair (2NE) in the spin-singlet and spin-triplet states. The second mechanism (B) is the pion exchange (PI) process where high momentum is transferred from the initial to the final proton by a virtual pion scattered off the intermediate deuteron that represents a pair of correlated nucleons. The last mechanism (C) is the direct proton-proton scattering (DIR). Another possible mechanism involving Δ-excitation is considered to be of little importance in the energy region of the present study.

The ^{3}He wave function is of special importance in the calculation of the reaction amplitudes. Full antisymmetric 3N wave functions were used [22] for the CD Bonn [23] and the Paris [24] potentials without the 3NF. The wave function was parametrized, restricted to the five partial wave components with the angular momentum of a nucleon pair in ^{3}He of $^1s_0$, $^3s_1$, and $^3d_1$ states, and the relative angular momentum of S and D waves between the pair and the residual nucleon. Within this restriction, the momentum distributions of a np

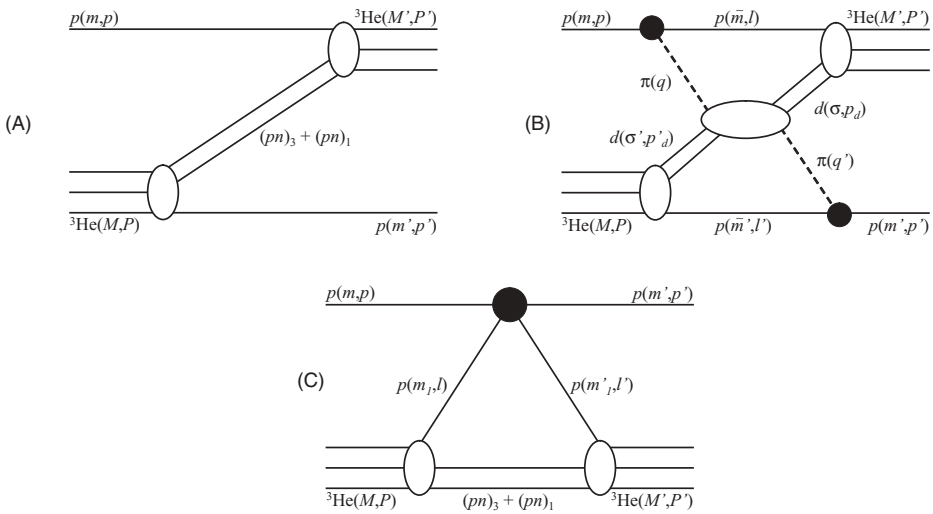

FIG. 4. Reaction mechanisms assumed for the $p+^3$He EBS at intermediate energy. The leftmost diagram (A) shows the 2NE, the middle diagram (B) the PI mechanism, and the rightmost diagram (C) the DIR mechanism. All the mechanisms are described in the text.

pair (both in the singlet and triplet states) and a deuteron in ^{3}He were calculated for comparison. At internal momenta $q < 300$ MeV/c, the spin-triplet pair exists mainly as a real deuteron for both above-mentioned potentials, suggesting a significant contribution of one deuteron exchange (ODE) processes in the 2NE mechanism and the justification for the assumption of the PI mechanism as seen in Fig. 4.

The three independent scattering amplitudes A, F, and G were formulated for each of the three reaction mechanisms. Using the momentum distributions of the two-nucleon pairs, the 2NE amplitudes were calculated with appropriate corrections for relativity in the infinite momentum frame (IMF) [25]. ODE and 2NE processes were calculated in the framework of light-cone dynamics. For the amplitude of subprocess of $\pi^0 d$ scattering appearing in the PI process, the results of the partial wave analysis of the elastic πd scattering by the Virginia group [26] were used. The coupling constant of the πNN vertex was taken from Ref. [27]. For the DIR process, we performed a calculation that minimizes the binding energy and the recoil correction. It employed the pp-scattering amplitude from the Saclay-Geneva partial wave analysis [28]. Combining the calculated reaction amplitudes we predicted the cross section and the spin-correlation parameter C_{yy} of the $\vec{p}+^3\vec{\text{He}}$ EBS.

IV. COMPARISON OF EXPERIMENTAL DATA WITH CALCULATION

We compare the measured differential cross sections and the spin correlation parameter C_{yy} in Figs. 5 and 6, respectively. The calculations are based on the ^{3}He wave function that were derived using the CD Bonn and the Paris potentials. In the figures, the open circles show the results of the present work. The other symbols are for the extrapolations of the data in Refs. [29–33] to 180°. The present data are consistent with the extrapolations.

For the differential cross section, the 2NE prediction is in good agreement with the data up to 200 MeV. Around 200–800 MeV, the inclusion of the DIR mechanism leads to a better agreement with the data. The contribution of the PI mechanism is found to be relatively small. The prediction including the ODE+PI+DIR mechanism slightly underestimates the data. The 2NE+PI+DIR predictions with both the CD Bonn and the Paris potentials represent well the measured energy dependence of the cross section. Although the calculations with CD Bonn and Paris potentials are very similar, the calculation with the CD Bonn potential reproduces the data slightly better than the calculation with the Paris potential. However, the calculations are too similar to determine which potential is preferred by the experiment.

For the spin correlation parameter C_{yy}, it must be noted that there are large discrepancies between the predictions from the 2NE+PI+DIR and the ODE+PI+DIR mechanisms. This clearly demonstrates the importance of the spin observables in studying the reaction mechanisms. The experimental result is obviously better described by the former calculation, showing that the continuum states of exchanged 2N system have important roles in the spin correlation parameter C_{yy}. The

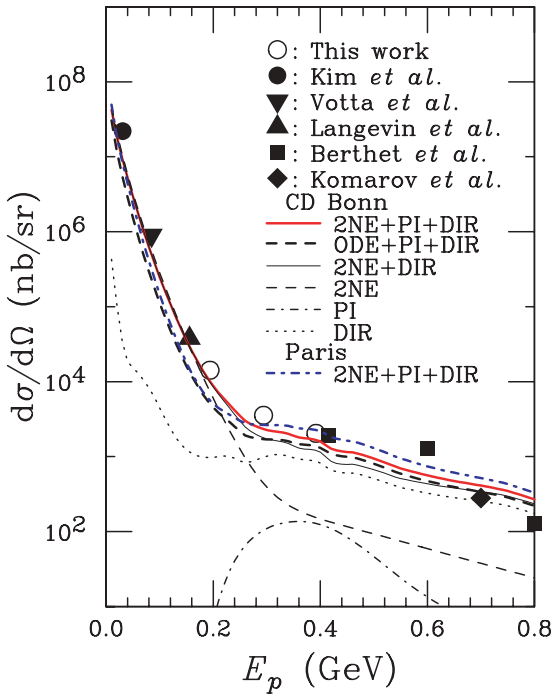

FIG. 5. (Color online) The differential cross section of the $p+^3$He EBS in the center-of-mass (c.m.) frame. Open circles show the results of this work, and the other data are the extrapolations to $\theta_{\text{c.m.}} = 180^\circ$ of data in Refs. [29] (closed circle), [30] (closed inverse triangle), [31] (closed triangle), [32] (closed square), and [33] (closed diamond). The bold solid (red) and bold dot-dashed (blue) curves represent 2NE+PI+DIR mechanisms with the ^{3}He wave function for the CD Bonn and the Paris potentials, respectively. The bold dashed, thin solid, thin dashed, dot-dashed, and dotted curves represent ODE+PI+DIR, 2NE+DIR, 2NE, PI, and DIR mechanism, respectively, with the ^{3}He wave function for the CD Bonn potential.

2NE+DIR prediction is also in good agreement with the data at 200 and 300 MeV but in rather poor agreement at 400 MeV. By including the PI mechanism, the prediction agrees much better with the data at 400 MeV but deviates from the data at 300 MeV. However, it has to be noted that the contribution of the PI mechanism is enhanced due to interferences with 2NE amplitudes in comparison to the case for the cross section. In the PI mechanism, only the subprocess $\pi^0 d \to \pi^0 d$ has been taken into account in the calculation. It might be necessary to modify the PI mechanism so as to include the subprocesses $\pi^0(pn)_1 \to \pi^0(pn)_1$, $\pi^0(pn)_3 \to \pi^0(pn)_3$, and $\pi^+(pp)_1 \to \pi^+(pp)_1$ as well. Such calculations would be of considerable interest.

In the present energy region, the 2NE mechanism gives an overall description of $\vec{p}+^3\vec{\text{He}}$ EBS. The reaction amplitudes of the 2NE process are given by momentum distributions of a virtual np pain in ^{3}He nucleus [13]. Momentum distributions consists of contributions from $^3s_1$ and $^3d_1$ states, interference between them and $^1s_0$ state, and they are calculated at the relativistic internal momentum, k_{IMF}, in the IMF [25]. At present energies of 200–400 MeV, the corresponding k_{IMF} is 0.33–0.48 GeV/c and the momentum distribution of $^3d_1$ state

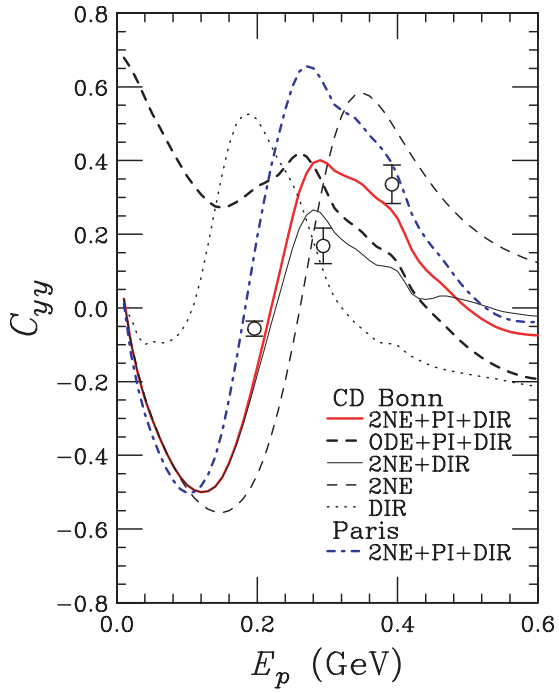

FIG. 6. (Color online) The spin correlation parameter C_{yy} of the p+^{3}He EBS. The same description as in the captions to Fig. 5 applies.

is much larger than that of $^3s_1$ and $^1s_0$ states. Remarkable differences between calculated C_{yy} with CD Bonn and Paris potentials reflect differences between $^3d_1$ wave functions. CD Bonn and Paris potentials give 7.1 and 8.4% of the D-state probability in the ^{3}He wave functions, respectively [22].

The calculation does not include the 3NF effects [34,35] and yet reproduces the differential cross section well. This may indicate that contributions of 3NF effects are small in the cross sections. We are very much interested in the calculation including the 3NF effects for the spin-correlation parameter C_{yy}.

V. SUMMARY AND CONCLUSIONS

The differential cross section and the spin correlation parameter C_{yy} of $\vec{p}$+$^3\vec{\text{He}}$ EBS have been measured at E_p = 200, 300, and 400 MeV to study the reaction mechanism and the validity of the ^{3}He wave function based on realistic 2N potentials. This is the first measurement of the spin-correlation parameter C_{yy} of the $\vec{p}$+$^3\vec{\text{He}}$ EBS at intermediate energies. For this purpose, a spin-exchange-polarized ^{3}He target was developed at RCNP. The maximum value of the ^{3}He polarization was 0.19. The measured differential cross sections were consistent with previous results extrapolated to $\theta_{\text{c.m.}} = 180^\circ$.

The experimental data were compared with theoretical predictions. For the differential cross section, the 2NE prediction was in good agreement with data up to 200 MeV. Around 200–800 MeV, the inclusion of the DIR mechanism led to a good agreement of the calculation with the data. The contribution of the PI mechanism was relatively small.

For the spin-correlation parameter C_{yy}, the 2NE+PI+DIR prediction clearly gave a better description of the data than the ODE+PI+DIR prediction at 200 MeV. This fact shows that the continuum states of the exchanged 2N system play an important role in the reaction. The 2NE+DIR prediction was also in good agreement with the data at 200 and 300 MeV but in rather poor agreement at 400 MeV. By including the PI mechanism, the prediction was in better agreement with the data at 400 MeV but it somewhat deviated from the data at 300 MeV. The contribution of the PI mechanism to the spin correlation parameter C_{yy} was found to be relatively large, as opposed to the better agreement for the cross sections. The calculations with the CD Bonn potential apparently describes the data better than those with the Paris potential for the spin-correlation parameter C_{yy}. The present work shows that the spin observables provide important information that cannot be obtained from the cross section alone. Although calculations by Kobushkin *et al.* do not included distortion effects in the entrance and exit channels and other reaction mechanisms, spin observables are generally less sensitive to distortion effects than the cross section. The spin-correlation parameter C_{zz} has a different dependence on the tensor scattering amplitudes from C_{yy}. To investigate the $\vec{p}$+$^3\vec{\text{He}}$ EBS in more detail, the measurement of both the spin correlation parameter C_{yy} and C_{zz} along with the further improvements of the theory are required.

The ^{3}He wave functions used in this work do not include 3NF effects, which should have an effect on high-momentum components in the wave function. Because of the high-momentum transfer, the EBS may provide a tool to investigate the 3NF effects in the ^{3}He wave function. It would, therefore, be interesting to calculate the EBS observables, including 3NF effects.

ACKNOWLEDGMENTS

We are indebted to the RCNP staff members for their supports during the experiment. We thank Professors S. Morinobu and G. P. A. Berg for their critical reading of the manuscript. This experiment was performed under program no. E180 at RCNP. This work was supported in part by the Grant-in-Aid for Scientific Research, grant no. 14340074, of the Ministry of Education, Culture, Sports, Science and Technology of Japan.

[1] C. F. Perdrisat *et al.*, Phys. Rev. Lett. **59**, 2840 (1987).
[2] V. Punjabi *et al.*, Phys. Rev. C **39**, 608 (1989).
[3] V. Punjabi *et al.*, Phys. Lett. **B350**, 178 (1995).
[4] V. G. Ableev *et al.*, Nucl. Phys. **A393**, 491 (1983).
[5] V. G. Ableev *et al.*, Few-Body Syst. **8**, 137 (1990).
[6] I. Sick, Prog. Part. Nucl. Phys. **47**, 245 (2001).

[7] M. B. Epstein *et al*., Phys. Rev. C **32**, 967 (1985) and references therein.
[8] M. A. Miller *et al*., Phys. Rev. Lett. **74**, 502 (1995).
[9] A. V. Lado and Yu. N. Uzikov, Phys. Lett. **B279**, 16 (1992).
[10] L. D. Blokhintsev, A. V. Lado, and Yu. N. Uzikov, Nucl. Phys. **A597**, 487 (1998).
[11] Yu. N. Uzikov, Nucl. Phys. **A644**, 321 (1998); Phys. Rev. C **58**, R36 (1998); Yu. N. Uzikov and J. Haidenbauer, *ibid*. **68**, 014001 (2003).
[12] A. Nakamura and L. Satta, Nucl. Phys. **A445**, 706 (1985).
[13] A. P. Kobushkin, E. A. Strokovsky, K. Hatanaka, and S. Ishikawa, nucl-th/0112078 (2001).
[14] K. Hatanaka, K. Takahisa, H. Tamura, M. Sato, and I. Miura, Nucl. Instrum. Methods Phys. Res. A **384**, 575 (1997).
[15] T. Wakasa *et al*., Nucl. Instrum. Methods Phys. Res. A **482**, 79 (2002).
[16] M. Fujiwara *et al*., Nucl. Instrum. Methods Phys. Res. A **422**, 484 (1999).
[17] M. A. Bouchiat, T. R. Carver, and C. M. Varnum, Phys. Rev. Lett. **5**, 373 (1960).
[18] G. G. Ohlsen, Rep. Prog. Phys. **35**, 717 (1972).
[19] Y. Shimizu *et al*., submitted to Nucl. Instrum. Methods Phys. Res. A.
[20] T. Noro *et al*., RCNP Annual Report 1991, p. 177.
[21] A. Tamii, H. Sakaguchi, H. Takeda, M. Yosoi, H. Akimune, M. Fujiwara, H. Ogata, M. Tanaka, and H. Togawa, IEEE Trans. Nucl. Sci. **43**, 2488 (1996); A. Tamii *et al*., in *Proceedings of the 2nd International Data Acquisition Workshop on Networked Data Acquisition System, Osaka, Japan, 1996*, edited by M. Nomachi and S. Ajimura (World Scientific, Singapore 1997), p. 238.
[22] V. Baru, J. Haidenbauer, C. Hanhart, and J. A. Niskanen, Eur. Phys. J. A **16**, 437 (2003).
[23] R. Machleidt, F. Sammarruca, and Y. Song, Phys. Rev. C **53**, R1483 (1996); R. Machleidt, Phys. Rev. C **63**, 024001 (2001); R. Machleidt and H. Müther, Phys. Rev. C **63**, 034005 (2001).
[24] M. Lacombe, B. Loiseau, J. M. Richard, R. Vinh Mau, J. Côté, P. Pirés, and R. de Tourreil, Phys. Rev. C **21**, 861 (1980).
[25] A. P. Kobushkin, J. Phys. G **12**, 487 (1986).
[26] R. A. Arndt, I. I. Strakovsky, and R. L. Workman, Phys. Rev. C **50**, 1796 (1994).
[27] R. Machleidt, K. Holinde, and Ch. Elster, Phys. Rep. **149**, 1 (1981).
[28] J. Bystricky, F. Lehar, and P. Winternitz, J. Phys. (Paris) **39**, 1 (1978); F. Lehar (private communication).
[29] C. C. Kim, S. M. Bunch, D. W. Devins, and H. H. Forster, Nucl. Phys. **58**, 32 (1964).
[30] L. G. Votta, P. G. Roos, N. S. Chant, and R. Woody, III, Phys. Rev. C **10**, 520 (1974).
[31] H. Langevin-Joliot, Ph. Narboni, J. P. Didelez, G. Duhamel, L. Marcus, and M. Roy-Stephan, Nucl. Phys. **A158**, 309 (1970).
[32] R. Frascaria *et al*., Phys. Lett. **B66**, 329 (1977).
[33] P. Berthet *et al*., Phys. Lett. **B106**, 465 (1981).
[34] S. A. Coon, M. D. Scadron, P. D. McNamee, B. R. Barrett, D. W. E. Blatt, and B. H. J. McKellar, Nucl. Phys. **A317**, 242 (1979); S. A. Coon and W. Glöckle, Phys. Rev. C **23**, 1790 (1981); S. A. Coon, Few-Body Syst. Suppl. **1**, 41 (1984); S. A. Coon and J. L. Friar, Phys. Rev. C **34**, 1060 (1986); S. A. Coon and M. T. Peña, Phys. Rev. C **48**, 2559 (1993).
[35] B. S. Pudliner, V. R. Pandharipande, J. Carlson, Steven C. Pieper, and R. B. Wiringa, Phys. Rev. C **56**, 1720 (1997).